Journal of Computational Physics 228 (2009) 9020–9035

Contents lists available at ScienceDirect

Journal of Computational Physics

journal homepage: www.elsevier.com/locate/jcp

A stable and conservative high order multi-block method for the compressible Navier–Stokes equations ☆

Jan Nordström [a,b,c,*], Jing Gong [c], Edwin van der Weide [d], Magnus Svärd [e]

[a] School of Mechanical, Industrial and Aeronautical Engineering, University of the Witvatersrand, PO WITS 2050, Johannesburg, South Africa
[b] Department of Aeronautics and Systems Integration, FOI, The Swedish Defense Research Agency, SE-164 90 Stockholm, Sweden
[c] Department of Information Technology, Scientific Computing, Uppsala University, SE-751 05 Uppsala, Sweden
[d] Faculty of Engineering Technology, University of Twente, P.O. Box 217, 7500 AE Enschede, The Netherlands
[e] Center of Mathematics for Applications, University of Oslo, P.B. 1053, Blindern, N-0316 Oslo, Norway

ARTICLE INFO

Article history:
Received 20 December 2008
Received in revised form 25 August 2009
Accepted 3 September 2009
Available online 15 September 2009

Keywords:
Navier–Stokes
Finite difference
High order
Stability
Conservation

ABSTRACT

A stable and conservative high order multi-block method for the time-dependent compressible Navier–Stokes equations has been developed. Stability and conservation are proved using summation-by-parts operators, weak interface conditions and the energy method. This development makes it possible to exploit the efficiency of the high order finite difference method for non-trivial geometries. The computational results corroborate the theoretical analysis.

1. Introduction

The high order finite difference method in combination with summation-by-parts operators and weak boundary conditions can very efficiently and reliably handle large problems on structured grids for reasonably smooth geometries. This has been shown in a sequence of papers, see for example [12,24,3,15,16,18,26,28]. The most recent papers [26,28] on this subject discuss the specific problem with far-field and no-slip boundaries. In this paper we will continue the development by treating the similar but not identical problem with a stable and accurate coupling of blocks.

In [4,23,29] the conventional (non-overlapping meshes) multi-block methodology is presented and discussed, but no theoretical analysis is performed. The stability of the non-overlapping multi-block techniques is analyzed in [5,14,6] using the one-dimensional normal mode analysis (see [10]). The overlapping grid technique has been studied in a similar manner using normal mode analysis in [2,21,22]. The analysis in the papers above is essentially one-dimensional (although a periodic behavior in the tangential direction can be included).

Due to the limitations of the normal mode analysis for multi-dimensional problems we will use the energy method in combination with summation-by-parts operators and weak boundary conditions as our theoretical tools. The technology in the two papers [26,28] together with the interface treatment in this paper will conclude the development of a high order accurate and truly stable multi-block finite difference method for the Navier–Stokes equations.

☆ This work was done while the first two authors were visiting CTR, The Center for Turbulence Research at Stanford University.

* Corresponding author. Address: School of Mechanical, Industrial and Aeronautical Engineering, University of the Witvatersrand, PO WITS 2050, Johannesburg, South Africa.
E-mail address: Jan.Nordstrom@foi.se (J. Nordström).

0021-9991/$ - see front matter © 2009 Elsevier Inc. All rights reserved.
doi:10.1016/j.jcp.2009.09.005

In the next phase of this development we will use the coupling technique developed in this paper and combine the high order finite difference method with the finite volume method in combination with unstructured grids which can more readily handle complex geometries. That development is ongoing, see for example [17,7,19]. The development in this paper is the theoretical foundation for that work.

The main challenge for multi-block methods is to control the possible instability at the block interfaces between sub-domains. We will focus on that problem and for *the first time* prove stability and conservation of a high order accurate multi-block finite difference method applied to the Navier–Stokes equations. The analysis will be done for the linear constant coefficient Navier–Stokes equations. The theoretical development is validated in numerical computations where the full non-linear Navier–Stokes equations are used.

The rest of the paper is organized as follows. In Section 2, we present the symmetric constant coefficient form of the Navier–Stokes equations followed by a short discussion of well-posedness in Section 3. The formulation of the numerical method on a single domain is considered in Section 4. The coupling procedure is the topic of Section 5 and the numerical experiments are presented in Section 6. Finally, conclusions are drawn in Section 7.

2. The Navier–Stokes equations

The frozen coefficient time-dependent compressible Navier–Stokes equations in two-dimensions in non-conservative form are given by, see [1]

$$\tilde{u}_t + A\tilde{u}_x + B\tilde{u}_y = C\tilde{u}_{xx} + D\tilde{u}_{xy} + E\tilde{u}_{xy}, \tag{1}$$

where $\tilde{u} = [\tilde{\rho}, \tilde{u}_1, \tilde{u}_2, \tilde{p}]^T$ and $A,\ B,\ C,\ D$, and E are coefficient matrices. $\tilde{\rho}$ is the density, $\tilde{u}_1$ and $\tilde{u}_2$ are the velocities and $\tilde{p}$ is the pressure. The coefficients are frozen at the constant state $u = [\rho, u_1, u_2, p]^T$. To apply the energy method we must symmetrize (1). The procedure developed in [1,20] yield a symmetric form of (1),

$$u_t + (A_1 u)_x + (A_2 u)_y = \varepsilon\Big[(B_{11}u_x + B_{12}u_y)_x + (B_{21}u_x + B_{22}u_y)_y\Big], \tag{2}$$

with $\varepsilon = 1/Re,\ u = \left(c\tilde{\rho}/(\sqrt{\gamma}\rho), \tilde{u}_1, \tilde{u}_2, \rho\tilde{T}/\sqrt{\gamma(\gamma-1)}\right)^T$ and

$$A_1 = \begin{bmatrix} u_1 & \frac{c}{\sqrt{\gamma}} & 0 & 0 \\ \frac{c}{\sqrt{\gamma}} & u_1 & 0 & \sqrt{\frac{\gamma-1}{\gamma}}c \\ 0 & 0 & u_1 & 0 \\ 0 & \sqrt{\frac{\gamma-1}{\gamma}}c & 0 & u_1 \end{bmatrix}, \quad A_2 = \begin{bmatrix} u_2 & 0 & \frac{c}{\sqrt{\gamma}} & 0 \\ 0 & u_2 & 0 & 0 \\ \frac{c}{\sqrt{\gamma}} & 0 & u_2 & \sqrt{\frac{\gamma-1}{\gamma}}c \\ 0 & 0 & \sqrt{\frac{\gamma-1}{\gamma}}c & u_2 \end{bmatrix}, \quad B_{11} = \begin{bmatrix} 0 & 0 & 0 & 0 \\ 0 & \frac{\lambda+2\mu}{\rho} & 0 & 0 \\ 0 & 0 & \frac{\mu}{\rho} & 0 \\ 0 & 0 & 0 & \frac{\gamma\mu}{\mathrm{Pr}\rho} \end{bmatrix},$$

$$B_{12} = B_{21} = \begin{bmatrix} 0 & 0 & 0 & 0 \\ 0 & 0 & \frac{\lambda+\mu}{2\rho} & 0 \\ 0 & \frac{\lambda+\mu}{2\rho} & 0 & 0 \\ 0 & 0 & 0 & 0 \end{bmatrix}, \quad B_{22} = \begin{bmatrix} 0 & 0 & 0 & 0 \\ 0 & \frac{\mu}{\rho} & 0 & 0 \\ 0 & 0 & \frac{\lambda+2\mu}{\rho} & 0 \\ 0 & 0 & 0 & \frac{\gamma\mu}{\mathrm{Pr}\rho} \end{bmatrix}.$$

In the vectors and matrices above we have used the temperature $\tilde{T}$, the ratio of the specific heats $\gamma = c_p/c_v$, the speed of sound c, the dynamic viscosity μ, the bulk viscosity λ, the kinematic viscosity $\nu = \mu/\rho$, the Prandtl number $\mathrm{Pr} = \nu/\alpha$ (α is the thermal diffusivity) and the Reynolds number $Re = \rho_\infty U_\infty L/\mu_\infty$. The infinity subscript denotes free stream conditions and L is a characteristic length. Note again that the form of the matrices (Jacobians) above are obtained for the symmetrized frozen coefficient version of the Navier–Stokes equations.

Eq. (2) can be rewritten in conservative form as

$$u_t + F_x + G_y = 0, \tag{3}$$

where

$$\begin{aligned} F &= A_1 u - \varepsilon(B_{11}u_x + B_{12}u_y) = F^I - \varepsilon F^V, \\ G &= A_2 u - \varepsilon(B_{21}u_x + B_{22}u_y) = G^I - \varepsilon G^V. \end{aligned} \tag{4}$$

F^I and G^I contain the inviscid terms and F^V and G^V the viscous terms.

3. Well-posedness of the continuous problem

To keep the algebraic complexity of the analysis as low as possible, we consider rectangular domains with Cartesian coordinates. Applying the energy method to (3) on the domain $\Omega \in [-1,1] \times [0,1]$ we obtain

$$\iint_\Omega u^T u_t \, dx\, dy + \iint_\Omega u^T F_x \, dx\, dy + \iint_\Omega u^T G_y \, dx\, dy = 0. \tag{5}$$

By using the Green–Gauss theorem, Eq. (5) can be written as

$$\frac{d}{dt}(\|u\|^2) = -\underbrace{\int_0^1 u^T(F^I - 2\varepsilon F^V)|_{x=1}\,dy}_{\text{East}} - \underbrace{\int_1^0 u^T(F^I - 2\varepsilon F^V)|_{x=-1}\,dy}_{\text{West}} - \underbrace{\int_{-1}^1 u^T(G^I - 2\varepsilon G^V)|_{y=0}\,dx}_{\text{South}} - \underbrace{\int_1^{-1} u^T(G^I - 2\varepsilon G^V)|_{y=1}\,dx}_{\text{North}}$$
$$- 2\varepsilon \iint_\Omega \begin{bmatrix} u_x \\ u_y \end{bmatrix}^T \underbrace{\begin{bmatrix} B_{11} & B_{12} \\ B_{21} & B_{22} \end{bmatrix}}_{B} \begin{bmatrix} u_x \\ u_y \end{bmatrix} dx\,dy. \tag{6}$$

To have a bounded energy growth, the boundary terms (East, West, North and South) must be bounded using the correct number and form of boundary conditions. That is the topic in papers [26,28] and it is not discussed further here. The contribution from the integral term is negative semi-definite since the matrix $B = [B_{11}\ B_{12}; B_{21}\ B_{22}]$ is positive semi-definite.

We summarize the result for the continuous problem (2)–(4) in the following proposition.

Proposition 3.1. *The continuous problem (2)–(4) is well posed if the boundary terms are limited by using the correct number of the boundary conditions.*

Remark. The n-dimensional Navier–Stokes equations require n boundary conditions at an inflow boundary and $n-1$ at an outflow boundary. In this case (two-dimensions) we need four boundary conditions an inflow boundary and three at an outflow boundary, see for example [25,10,20].

4. Stability on a single domain

Consider the computational domain with a Cartesian mesh of $(M+1)\times(N+1)$ points. Let the kth element of the continuous variable u at the structured grid point (x_i, y_j) be $u(i,j,k)$ $(0 \leqslant k \leqslant 3)$. The finite difference approximation of $u(i,j,k)$ is collected in a global vector $\mathbf{v}$ such that $v[4i(N+1+4j+k)] = u(i,j,k)$ $(0 \leqslant i \leqslant M, 0 \leqslant j \leqslant N$ and $0 \leqslant k \leqslant 3)$. Let $\mathbf{v}_x$ and $\mathbf{v}_y$ be approximations of u_x and u_y.

By using the finite difference method developed in [12,24,3,15,16,18,26,28] a semi-discrete approximation of Eq. (3) can be written as

$$\mathbf{v}_t + D_x\mathbf{F} + D_y\mathbf{G} = 0, \tag{7}$$

where $D_x = P_x^{-1}Q_x \otimes I_y \otimes I_4$ and $D_y = I_x \otimes P_y^{-1}Q_y \otimes I_4$ are first derivative operators in x- and y-directions, respectively. I_x and I_y are the identity matrices of size $(M+1)\times(M+1)$ and $(N+1)\times(N+1)$. Moreover,

$$\mathbf{F} = \mathbf{F}^I - \varepsilon\mathbf{F}^V, \quad \mathbf{G} = \mathbf{G}^I - \varepsilon\mathbf{G}^V$$
$$\mathbf{F}^I = (I_x \otimes I_y \otimes A_1)\mathbf{v}, \quad \mathbf{F}^V = (I_x \otimes I_y \otimes B_{11})\mathbf{v}_x + (I_x \otimes I_y \otimes B_{12})\mathbf{v}_y,$$
$$\mathbf{G}^I = (I_x \otimes I_y \otimes A_2)\mathbf{v}, \quad \mathbf{G}^V = (I_x \otimes I_y \otimes B_{21})\mathbf{v}_x + (I_x \otimes I_y \otimes B_{22})\mathbf{v}_y,$$

and $\mathbf{v}_x = D_x\mathbf{v}$, $\mathbf{v}_y = D_y\mathbf{v}$. Let $\overline{P} = P_x \otimes P_y$ and multiply Eq. (7) with $\mathbf{v}^T(\overline{P} \otimes I_4)$. (This is the discrete equivalent of multiplying (3) with v^T and integrating over the computational domain to get the energy estimate (6).)

This leads to

$$\mathbf{v}^T(\overline{P} \otimes I_4)\mathbf{v}_t + \mathbf{v}^T(Q_x \otimes P_y \otimes I_4)\mathbf{F} + \mathbf{v}^T(P_x \otimes Q_y \otimes I_4)\mathbf{G} = 0. \tag{8}$$

By adding the transpose of Eq. (8) to itself and using the SBP relations

$$Q_x + Q_x^T = \mathrm{diag}(-1, 0, \ldots, 0, 1), \quad Q_y + Q_y^T = \mathrm{diag}(-1, 0, \ldots, 0, 1), \tag{9}$$

we can write the result as

$$\frac{d}{dt}\left(\|\mathbf{v}\|^2_{\overline{P}\otimes I_4}\right) = -\mathrm{IT} + \varepsilon\mathrm{VT}. \tag{10}$$

The inviscid term IT in (10) is

$$\mathrm{IT} = \mathbf{v}^T(Q_x \otimes P_y \otimes I_4)\mathbf{F}^I + (\mathbf{F}^I)^T\left(Q_x^T \otimes P_y \otimes I_4\right)\mathbf{v} + \mathbf{v}^T(P_x \otimes Q_y \otimes I_4)\mathbf{G}^I + (\mathbf{G}^I)^T\left(P_x \otimes Q_y^T \otimes I_4\right)\mathbf{v}$$
$$= \underbrace{\mathbf{v}_E^T(P_y \otimes I_4)\mathbf{F}_E^I}_{\text{East}} - \underbrace{\mathbf{v}_W^T(P_y \otimes I_4)\mathbf{F}_W^I}_{\text{West}} - \underbrace{\mathbf{v}_S^T(P_x \otimes I_4)\mathbf{G}_S^I}_{\text{South}} + \underbrace{\mathbf{v}_N^T(P_x \otimes I_4)\mathbf{G}_N^I}_{\text{North}}. \tag{11}$$

The viscous term VT in (10) can be written as

$$\mathrm{VT} = \mathbf{v}^T(Q_x \otimes P_y \otimes I_4)\mathbf{F}^V + (\mathbf{F}^V)^T\left(Q_x^T \otimes P_y \otimes I_4\right)\mathbf{v} + \mathbf{v}^T(P_x \otimes Q_y \otimes I_4)\mathbf{G}^V + (\mathbf{G}^V)^T(P_x \otimes Q_y \otimes I_4)^T\mathbf{v}$$
$$= 2\underbrace{\mathbf{v}_E^T(P_y \otimes I_4)\mathbf{F}_E^V}_{\text{East}} - 2\underbrace{\mathbf{v}_W^T(P_y \otimes I_4)\mathbf{F}_W^V}_{\text{West}} - 2\underbrace{\mathbf{v}_S^T(P_x \otimes I_4)\mathbf{G}_S^V}_{\text{South}} + 2\underbrace{\mathbf{v}_N^T(P_x \otimes I_4)\mathbf{G}_N^V}_{\text{North}} - 2\begin{bmatrix} \mathbf{v}_x \\ \mathbf{v}_y \end{bmatrix}^T \begin{bmatrix} \overline{P} \otimes B_{11} & \overline{P} \otimes B_{12} \\ \overline{P} \otimes B_{21} & \overline{P} \otimes B_{22} \end{bmatrix} \begin{bmatrix} \mathbf{v}_x \\ \mathbf{v}_y \end{bmatrix}. \tag{12}$$

An expanded version of Eq. (10) using the relations above becomes

$$\frac{d}{dt}\left(\|\mathbf{v}\|^2_{\overline{P}\otimes I_4}\right) = -\underbrace{\mathbf{v}_E^T(P_y\otimes I_4)(\mathbf{F}_E^I - 2\varepsilon\mathbf{F}_E^V)}_{\text{East}} + \underbrace{\mathbf{v}_W^T(P_y\otimes I_4)(\mathbf{F}_W^I - 2\varepsilon\mathbf{F}_W^V)}_{\text{West}} + \underbrace{\mathbf{v}_S^T(P_x\otimes I_4)(\mathbf{G}_S^I - 2\varepsilon\mathbf{G}_S^V)}_{\text{South}} - \underbrace{\mathbf{v}_N^T(P_x\otimes I_4)(\mathbf{G}_N^I - 2\varepsilon\mathbf{G}_N^V)}_{\text{North}}$$
$$- 2\varepsilon\begin{bmatrix}\mathbf{v}_x\\ \mathbf{v}_y\end{bmatrix}^T\begin{bmatrix}\overline{P}\otimes B_{11} & \overline{P}\otimes B_{12}\\ \overline{P}\otimes B_{21} & \overline{P}\otimes B_{22}\end{bmatrix}\begin{bmatrix}\mathbf{v}_x\\ \mathbf{v}_y\end{bmatrix}. \tag{13}$$

Note that for square matrices $\overline{P}$ and B_{11} (or B_{12}, B_{21} and B_{22}) the Kronecker product $\overline{P}\otimes B_{11}$ and $B_{11}\otimes\overline{P}$ are even permutation similar, that is, there exists a permutation matrix Φ such that $\overline{P}\otimes B_{11} = \Phi^T(B_{11}\otimes\overline{P})\Phi$, see [11] for details. Eq. (13) can therefore be written

$$\frac{d}{dt}\left(\|\mathbf{v}\|^2_{\overline{P}\otimes I_4}\right) = \mathrm{BT} - 2\varepsilon\begin{bmatrix}\mathbf{w}_x\\ \mathbf{w}_y\end{bmatrix}^T\begin{bmatrix}B_{11} & B_{12}\\ B_{21} & B_{22}\end{bmatrix}\otimes\overline{P}\begin{bmatrix}\mathbf{w}_x\\ \mathbf{w}_y\end{bmatrix}, \tag{14}$$

where BT collect all the boundary terms in (13) and $\mathbf{w}_x = \Phi\mathbf{v}_x$, $\mathbf{w}_y = \Phi\mathbf{v}_y$.

Exactly similar to the continuous case, a bounded energy growth in (14) require boundedness in terms of given data of the boundary terms (East, West, North and South). Again, that is dealt with in the papers [26,28] where the boundary conditions are implemented using penalty terms. The contribution from the quadratic form in (14) is negative semi-definite since the matrix $\overline{P}$ is positive definite and $B = [B_{11}\ B_{12}; B_{21}\ B_{22}]$ is positive semi-definite.

Exactly similar to the continuous case, we summarize the result for the semi-discrete single domain problem (7) in the following proposition.

Proposition 4.1. *The semi-discrete problem (7) is stable if the boundary terms are limited by appropriate boundary procedures.*

5. Stable and conservative interface conditions

We consider a computational domain consisting of two sub-domains and a common interface at $x = 0$, see Fig. 1. Let $\mathbf{u}$ and $\mathbf{v}$ be the unknowns in the left and right sub-domain, respectively, and introduce the superscripts L and R to identify the left and right sub-domains.

The semi-discrete approximation of (2) on the two sub-domains with an interface can be written

$$\mathbf{u}_t + D_x^L\mathbf{F}^L + D_y^L\mathbf{G}^L = (M^L)^{-1}\left(\overline{\Sigma}_1^L[\mathbf{u}_i - \mathbf{v}_i] + \overline{\Sigma}_2^L\left[(\mathbf{F}^V)_i^L - (\mathbf{F}^V)_i^R\right]\right), \tag{15a}$$

$$\mathbf{v}_t + D_x^R\mathbf{F}^R + D_y^R\mathbf{G}^R = (M^R)^{-1}\left(\overline{\Sigma}_1^R[\mathbf{v}_i - \mathbf{u}_i] + \overline{\Sigma}_2^R\left[(\mathbf{F}^V)_i^R - (\mathbf{F}^V)_i^L\right]\right), \tag{15b}$$

where the matrices E^L, E^R picks out the parts of the vectors residing at the interface such that for example $\mathbf{u}_i = E^L\mathbf{u}$, $\mathbf{v}_i = E^R\mathbf{v}$. In the following, the subscript i indicates that the quantity resides on the interface. We also have the definitions:

$$\begin{aligned}
&D_x^L = \left(P_x^L\right)^{-1}Q_x^L\otimes I_y^L\otimes I_4, \quad D_y^L = I_x^L\otimes\left(P_y^L\right)^{-1}Q_y^L\otimes I_4,\\
&D_x^R = \left(P_x^R\right)^{-1}Q_x^R\otimes I_y^R\otimes I_4, \quad D_y^R = I_x^R\otimes\left(P_y^R\right)^{-1}Q_y^R\otimes I_4,\\
&M^L = P_x^L\otimes P_y^L\otimes I_4, \quad M^R = P_x^R\otimes P_y^R\otimes I_4,\\
&\overline{\Sigma}_1^L = (E^L)^TP_y^L\otimes\Sigma_1^L, \quad \overline{\Sigma}_2^L = (E^L)^TP_y^L\otimes\Sigma_2^L,\\
&\overline{\Sigma}_1^R = (E^R)^TP_y^R\otimes\Sigma_1^R, \quad \overline{\Sigma}_2^R = (E^R)^TP_y^R\otimes\Sigma_2^R.
\end{aligned} \tag{16}$$

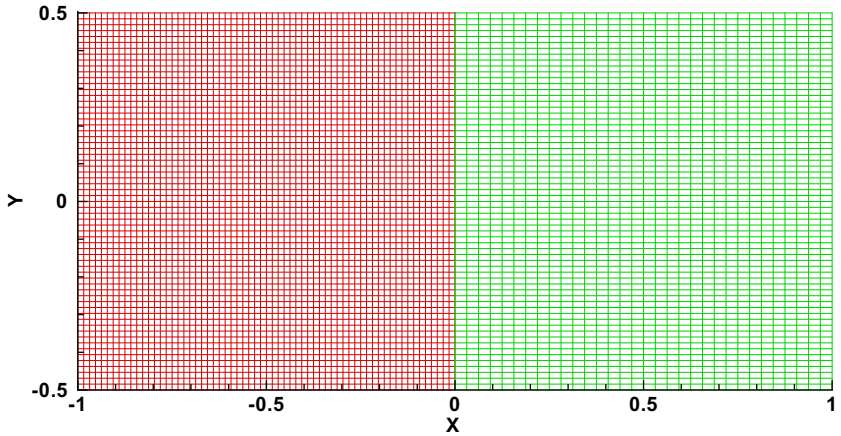

Fig. 1. A hybrid mesh of $65\times 65 + 33\times 65$ grid points.

The definitions of **F** and **G** are given in Section 4 above and $\Sigma_1^L,\ \Sigma_1^R,\ \Sigma_2^L,\ \Sigma_2^R$ unknown penalty matrices. Note that the outer boundary conditions are neglected in this analysis, for separate treatment of these see [26,28].

We will determine the penalty matrices $\Sigma_1^L,\ \Sigma_1^R,\ \Sigma_2^L,\ \Sigma_2^R$ by stability and conservation requirements (see [3,15,16,18] for previous applications of this technique). Applying the energy method to (15a) and (15b) yields

$$\frac{d}{dt}\left(\|\mathbf{u}\|_{M^L}^2+\|\mathbf{v}\|_{M^R}^2\right)+2\varepsilon\,\mathrm{Diss}=\mathbf{w}_i^T M\mathbf{w}_i, \tag{17}$$

where $\mathbf{w}_i=[\mathbf{u}_i,\mathbf{v}_i,(\mathbf{u}_x)_i,(\mathbf{v}_x)_i,(\mathbf{u}_y)_i,(\mathbf{v}_y)_i]^T$ and

$$\mathrm{Diss}=\begin{bmatrix}\mathbf{u}_x\\ \mathbf{u}_y\end{bmatrix}^T\begin{bmatrix}P_x^L\otimes P_y^L\otimes B_{11} & P_x^L\otimes P_y^L\otimes B_{12}\\ P_x^L\otimes P_y^L\otimes B_{21} & P_x^L\otimes P_y^L\otimes B_{22}\end{bmatrix}\begin{bmatrix}\mathbf{u}_x\\ \mathbf{u}_y\end{bmatrix}+\begin{bmatrix}\mathbf{v}_x\\ \mathbf{v}_y\end{bmatrix}^T\begin{bmatrix}P_x^R\otimes P_y^R\otimes B_{11} & P_x^R\otimes P_y^R\otimes B_{12}\\ P_x^R\otimes P_y^R\otimes B_{21} & P_x^R\otimes P_y^R\otimes B_{22}\end{bmatrix}\begin{bmatrix}\mathbf{v}_x\\ \mathbf{v}_y\end{bmatrix}.$$

The matrix M in (17) determines the stability of the interface treatment. M is symmetric and the elements of M are

$$\begin{aligned}
&M_{11}=P_y^L\otimes\left(-A_1+\Sigma_1^L+\left(\Sigma_1^L\right)^T\right),\quad M_{12}=P_y^L\otimes-\Sigma_1^L+P_y^R\otimes-\left(\Sigma_1^R\right)^T,\\
&M_{13}=P_y^L\otimes\left(\varepsilon I_4+\Sigma_2^L\right)B_{11},\quad M_{14}=P_y^L\otimes-\Sigma_2^L B_{11},\\
&M_{15}=P_y^L\otimes\left(\varepsilon I_4+\Sigma_2^L\right)B_{12},\quad M_{16}=P_y^L\otimes-\Sigma_2^L B_{12},\\
&M_{22}=P_y^R\otimes\left(A_1+\Sigma_1^R+\left(\Sigma_1^R\right)^T\right),\quad M_{23}=P_y^R\otimes-\Sigma_2^R B_{11},\\
&M_{24}=P_y^L\otimes\left(-\varepsilon I_4+\Sigma_2^R\right)B_{11},\quad M_{25}=P_y^L\otimes-\Sigma_2^R B_{12},\\
&M_{26}=P_y^R\otimes\left(-\varepsilon I_4+\Sigma_2^R\right)B_{12},\quad M_{33}=M_{34}=M_{35}=M_{36}=0,\\
&M_{44}=M_{45}=M_{46}=0,\quad M_{55}=M_{56}=M_{66}=0.
\end{aligned}$$

Notice that the matrix M in its present form is indefinite.

In order to construct a symmetric semi-definite negative matrix on the right-hand side of Eq. (17) we must "borrow" interface terms from Diss on the left-hand side, see [3]. The term Diss can be written as

$$\mathrm{Diss}=\widetilde{\mathrm{Diss}}+\alpha^L p^L\begin{bmatrix}(\mathbf{u}_x)_i\\ (\mathbf{u}_y)_i\end{bmatrix}^T\begin{bmatrix}P_y^L\otimes B_{11} & P_y^L\otimes B_{12}\\ P_y^L\otimes B_{21} & P_y^L\otimes B_{22}\end{bmatrix}\begin{bmatrix}(\mathbf{u}_x)_i\\ (\mathbf{u}_y)_i\end{bmatrix}+\beta^R p^R\begin{bmatrix}(\mathbf{v}_x)_i\\ (\mathbf{v}_y)_i\end{bmatrix}^T\begin{bmatrix}P_y^R\otimes B_{11} & P_y^R\otimes B_{12}\\ P_y^R\otimes B_{21} & P_y^R\otimes B_{22}\end{bmatrix}\begin{bmatrix}(\mathbf{v}_x)_i\\ (\mathbf{v}_y)_i\end{bmatrix}$$

where $p^L=\left(P_x^L\right)_{M,M}$, $p^R=\left(P_x^R\right)_{1,1}$ and

$$\widetilde{\mathrm{Diss}}=\begin{bmatrix}\mathbf{u}_x\\ \mathbf{u}_y\end{bmatrix}^T\begin{bmatrix}\widetilde{P_x^L}\otimes P_y^L\otimes B_{11} & \widetilde{P_x^L}\otimes P_y^L\otimes B_{12}\\ \widetilde{P_x^L}\otimes P_y^L\otimes B_{21} & \widetilde{P_x^L}\otimes P_y^L\otimes B_{22}\end{bmatrix}\begin{bmatrix}\mathbf{u}_x\\ \mathbf{u}_y\end{bmatrix}+\begin{bmatrix}\mathbf{v}_x\\ \mathbf{v}_y\end{bmatrix}^T\begin{bmatrix}\widetilde{P_x^R}\otimes P_y^R\otimes B_{11} & \widetilde{P_x^R}\otimes P_y^R\otimes B_{12}\\ \widetilde{P_x^R}\otimes P_y^R\otimes B_{21} & \widetilde{P_x^R}\otimes P_y^R\otimes B_{22}\end{bmatrix}\begin{bmatrix}\mathbf{v}_x\\ \mathbf{v}_y\end{bmatrix}.$$

The modified norms in $\widetilde{\mathrm{Diss}}$ are $\widetilde{P_x^L}=P_x^L-\mathrm{diag}(0,\ldots,\alpha^L p^L)$ and $\widetilde{P_x^R}=P_x^R-\mathrm{diag}(\beta^R p^R,0,\ldots,0)$. Note that with $0<\alpha^L,\ \beta^R\leqslant 1$, then $\widetilde{P_x^L}\geqslant 0$ and $\widetilde{P_x^R}\geqslant 0$ and hence $\widetilde{\mathrm{Diss}}\geqslant 0$.

As a result, the modified version of Eq. (17) can be written as

$$\frac{d}{dt}\left(\|\mathbf{u}\|_{M^L}^2+\|\mathbf{v}\|_{M^R}^2\right)+2\varepsilon\,\widetilde{\mathrm{Diss}}=\mathbf{w}_i^T\widetilde{M}\mathbf{w}_i, \tag{18}$$

where $\widetilde{M}$ plays the role of M except that the zero elements in M are replaced by

$$\begin{aligned}
&M_{33}=-2\varepsilon\alpha^L p^L P_y^L\otimes B_{11},\quad M_{35}=-2\varepsilon\alpha^L p^L P_y^L\otimes B_{12},\\
&M_{44}=-2\varepsilon\beta^R p^R P_y^R\otimes B_{11},\quad M_{46}=-2\varepsilon\beta^R p^R P_y^R\otimes B_{12},\\
&M_{55}=-2\varepsilon\alpha^L p^L P_y^L\otimes B_{22},\quad M_{66}=-2\varepsilon\beta^R p^R P_y^R\otimes 2B_{22},\\
&M_{53}=M_{35}^T,\quad M_{64}=M_{46}^T.
\end{aligned}$$

5.1. Conservation conditions

Before considering the stability, we investigate the conservation properties at the interface. Let φ be a smooth test function with compact support, multiply Eq. (3) with φ and integrate over the spatial domain $\Omega\in[-1,1]\times[0,1]$. We obtain

$$\iint_\Omega \varphi^T u_t\,dx\,dy-\iint_\Omega\left(\varphi_x^T F+\varphi_y^T G\right)dx\,dy=0. \tag{19}$$

The conservative form of Eq. (3) makes it possible to use integration-by-parts and move the differentiation on to the smooth continuous function φ.

We want to preserve this property in the discrete case. For the single domain problem this is trivial since the SBP operators are constructed to do just that, see Eq. (9). However, in the multi-domain case we have an interface and extra care is necessary.

With a slight abuse of notation we also let φ denote a smooth grid function. Note that this means that $\varphi_i^L = \varphi_i^R = \varphi_i$. Multiplying Eqs. (15a) and (15b) by $(\varphi^T M)^L$ and $(\varphi^T M)^R$, respectively, and using the SBP relations (9) leads to

$$(\varphi^T M)^L \mathbf{u}_t + (\varphi^T M)^R \mathbf{v}_t - \left(\varphi_x^T M \mathbf{F} + \varphi_y^T M \mathbf{G}\right)^L - \left(\varphi_x^T M \mathbf{F} + \varphi_y^T M \mathbf{G}\right)^R = \mathrm{IT}. \tag{20}$$

The M^L, M^R involved in (20) are defined in (16). The left-hand side of (20) corresponds exactly to the left-hand side of (19). As usual we have neglected the outer boundary terms.

If the interface term IT at the right-hand side of (20) vanish, we have a conservative scheme. The interface term is

$$\begin{aligned}\mathrm{IT} = \varphi_i^T \Big[&-\left(P_y^L \otimes A_1\right)\mathbf{u}_i + \left(P_y^R \otimes A_1\right)\mathbf{v}_i + \left(P_y^L \otimes \Sigma_1^L - P_y^R \otimes \Sigma_1^R\right)(\mathbf{u}_i - \mathbf{v}_i) + \left(P_y^L \otimes \varepsilon I_4\right)\left(\mathbf{F}_i^V\right)^L - \left(P_y^R \otimes \varepsilon I_4\right)\left(\mathbf{F}_i^V\right)^R \\ &+\left(P_y^L \otimes \Sigma_1^L - P_y^R \otimes \Sigma_1^R\right)\left((\mathbf{F}_i^V)^L - \left(\mathbf{F}_i^V\right)^R\right)\Big].\end{aligned}$$

The choice $P_y^L = P_y^R$ and the conditions (21) below cancel the interface term IT in (20) and lead to a conservative scheme:

$$\Sigma_1^R = \Sigma_1^L - A_1, \quad \Sigma_2^R = \Sigma_2^L + \varepsilon I_4. \tag{21}$$

Remark. The conservation conditions (21) are a subset of the resulting stability conditions, see also [3,15,16,18] where similar conservation conditions were derived.

Remark. The condition $P_y^L = P_y^R$ implies that the same SBP operators should be used in the y-direction in both sub-domains. This restriction can be removed, and that will be the topic in a future paper.

5.2. Stability conditions

Inserting $P_y^L = P_y^R = P_y$ and the conservation conditions (21) into (18) results in

$$\frac{d}{dt}\left(\|\mathbf{u}\|_{M^L}^2 + \|\mathbf{v}\|_{M^R}^2\right) + 2\varepsilon\,\widetilde{\mathrm{Diss}} = -\mathbf{x}^T (N \otimes P_y)\mathbf{x}, \tag{22}$$

where

$$\mathbf{x} = \begin{bmatrix} \Phi\mathbf{u} \\ \Psi\mathbf{v} \\ \Phi\mathbf{u}_x \\ \Psi\mathbf{v}_x \\ \Phi\mathbf{u}_y \\ \Psi\mathbf{v}_y \end{bmatrix}, \quad N = \begin{bmatrix} N_{11} & -N_{11} & N_{13} & N_{14} & N_{15} & N_{16} \\ -N_{11} & N_{11} & -N_{13} & -N_{14} & -N_{15} & -N_{16} \\ N_{13}^T & -N_{13}^T & N_{33} & 0 & N_{35} & 0 \\ N_{14}^T & -N_{14}^T & 0 & N_{44} & 0 & N_{46} \\ N_{15}^T & -N_{15}^T & N_{35}^T & 0 & N_{55} & 0 \\ N_{16}^T & -N_{16}^T & 0 & N_{46}^T & 0 & N_{66} \end{bmatrix}.$$

The permutation matrices Φ and Ψ are defined in Section 4 and

$$\begin{aligned} &N_{11} = \left(A_1 - \Sigma_1^L - \left(\Sigma_1^L\right)^T\right), \quad N_{13} = -\left(\varepsilon I_4 + \Sigma_2^L\right)B_{11}, \quad N_{14} = \Sigma_2^L B_{11}, \\ &N_{15} = -\left(\varepsilon I_4 + \Sigma_2^L\right)B_{12}, \quad N_{16} = \Sigma_2^L B_{12}, \quad N_{33} = 2\varepsilon\alpha^L p^L B_{11}, \\ &N_{35} = 2\varepsilon\alpha^L p^L B_{12}, \quad N_{44} = 2\varepsilon\beta^R p^R B_{11}, \quad N_{46} = 2\varepsilon\beta^R p^R B_{12}, \\ &N_{55} = 2\varepsilon\alpha^L p^L B_{22}, \quad N_{66} = 2\varepsilon\beta^R p^R B_{22}. \end{aligned}$$

A bounded energy require a positive semi-definite matrix N. To simplify the algebra we introduce a transformation matrix S such that $S^T S = I$ and

$$S = \begin{bmatrix} \frac{1}{\sqrt{2}}I_4 & \frac{1}{\sqrt{2}}I_4 & 0 & 0 & 0 & 0 \\ 0 & 0 & I_4 & 0 & 0 & 0 \\ 0 & 0 & 0 & 0 & I_4 & 0 \\ 0 & 0 & 0 & I_4 & 0 & 0 \\ 0 & 0 & 0 & 0 & 0 & I_4 \\ \frac{1}{\sqrt{2}}I_4 & -\frac{1}{\sqrt{2}}I_4 & 0 & 0 & 0 & 0 \end{bmatrix}, \quad \widehat{N} = SNS^T = \begin{bmatrix} 0 & 0 & 0 & 0 & 0 & 0 \\ 0 & N_{33} & N_{35} & 0 & 0 & \sqrt{2}N_{13} \\ 0 & N_{35}^T & N_{55} & 0 & 0 & \sqrt{2}N_{15} \\ 0 & 0 & 0 & N_{44} & N_{46} & \sqrt{2}N_{14} \\ 0 & 0 & 0 & N_{46}^T & N_{66} & \sqrt{2}N_{16} \\ 0 & \sqrt{2}N_{13}^T & \sqrt{2}N_{15}^T & \sqrt{2}N_{14}^T & \sqrt{2}N_{16}^T & 2N_{11} \end{bmatrix}$$

To simplify the matrix $\widehat{N}$ we introduce

$$\alpha = \alpha^L p^L, \quad \beta = \beta^R p^R, \quad \Sigma_2^L = -\varepsilon\Lambda, \quad \Sigma_1^L = \Sigma_{1I}^L + \varepsilon\Sigma_{1V}^L, \tag{23}$$

where we choose Λ to be diagonal. The splitting and scaling with ε in (23) are made for convenience and means that $\widehat{N}$ can be split into an inviscid part $\widehat{N}_I$ and a viscous part $\widehat{N}_V$ which simplifies the analysis. By making use of (23) we get

$$\widehat{N} = \underbrace{\begin{bmatrix} \mathbf{0}_{20,20} & \mathbf{0}_{20,4} \\ \mathbf{0}_{4,20} & 2\left(A_1 - \Sigma_{1I}^L - \left(\Sigma_{1I}^L\right)^T\right) \end{bmatrix}}_{\widehat{N}_I} + \varepsilon \underbrace{\begin{bmatrix} \mathbf{0}_{4,4} & \mathbf{0}_{4,8} & \mathbf{0}_{4,8} & \mathbf{0}_{4,4} \\ \mathbf{0}_{8,4} & 2\alpha K_{11} & \mathbf{0}_{8,8} & \sqrt{2}K_{13} \\ \mathbf{0}_{8,4} & \mathbf{0}_{8,8} & 2\beta K_{11} & \sqrt{2}K_{23} \\ \mathbf{0}_{4,4} & \sqrt{2}K_{13}^T & \sqrt{2}K_{23}^T & 2K_{33} \end{bmatrix}}_{\widehat{N}_V}, \tag{24}$$

where $K_{33} = -(\Sigma_{1V} + (\Sigma_{1V})^T)$ and

$$K_{11} = \begin{bmatrix} B_{11} & B_{12} \\ B_{21} & B_{22} \end{bmatrix}, \quad K_{13} = \begin{bmatrix} (\Lambda - I_4)B_{11} \\ (\Lambda - I_4)B_{12} \end{bmatrix}, \quad K_{23} = \begin{bmatrix} -\Lambda B_{11} \\ -\Lambda B_{12} \end{bmatrix}.$$

The subscripts on $\mathbf{0}$ in (24) indicate the size of the block.

The condition for $\widehat{N}_I$ in Eq. (24) to be positive semi-definite is

$$A_1 - \Sigma_{1I}^L - \left(\Sigma_{1I}^L\right)^T \geqslant 0. \tag{25}$$

If A_1 is rewritten as $A_1 = X^T\Lambda X = X^T\Lambda^+ X + X^T\Lambda^- X = A_1^+ + A_1^-$ where $\Lambda^+ = \mathrm{diag}(\max(\lambda_i, 0))$, $\Lambda^- = \mathrm{diag}(\min(\lambda_i, 0))$ and λ_i are the eigenvalues of A_1, we find that (25) is satisfied if

$$\Sigma_{1I}^L + \left(\Sigma_{1I}^L\right)^T \leqslant A_1^-. \tag{26}$$

Next we turn to the more difficult analysis of the definiteness of $\widehat{N}_V$. The dimensions of $\widehat{N}_V$ and the matrices K_{11}, K_{13}, K_{23} and K_{33} are given in (24). Note that since the matrices B_{ij} all lack the first row and column, the only non-zero part of $\widehat{N}_V$ that we need to consider for definiteness is the condensed version (we neglect the rows and columns that consist of zeros) of the lower 3×3 block in (24).

Let us denote the condensed version of the lower 3×3 block in $\widehat{N}_V$ with $\widetilde{N}$ and use a similar notation also for the rest of the matrices. That means that we should consider definiteness of

$$\widetilde{N} = \begin{bmatrix} 2\alpha\widetilde{K}_{11} & \mathbf{0}_{6,6} & \sqrt{2}\widetilde{K}_{13} \\ \mathbf{0}_{6,6} & 2\beta\widetilde{K}_{11} & \sqrt{2}\widetilde{K}_{23} \\ \sqrt{2}\widetilde{K}_{13}^T & \sqrt{2}\widetilde{K}_{23}^T & 2\widetilde{K}_{33} \end{bmatrix}, \quad \widetilde{K}_{33} = -(\Sigma + \Sigma^T) \tag{27}$$

$$\widetilde{K}_{11} = \begin{bmatrix} \widetilde{B}_{11} & \widetilde{B}_{12} \\ \widetilde{B}_{21} & \widetilde{B}_{22} \end{bmatrix}, \quad \widetilde{K}_{13} = \begin{bmatrix} (\Lambda - I_3)\widetilde{B}_{11} \\ (\Lambda - I_3)\widetilde{B}_{12} \end{bmatrix}, \quad \widetilde{K}_{23} = \begin{bmatrix} -\Lambda\widetilde{B}_{11} \\ -\Lambda\widetilde{B}_{12} \end{bmatrix}. \tag{28}$$

Note again that we have now replaced all 4×4 matrices with the corresponding 3×3 ones. We have also kept the notation Λ and changed Σ_{1V} to Σ.

We find that a sufficient condition for positive semi-definiteness of $\widetilde{N}$ is

$$\widetilde{K}_{11} > 0 \quad \text{and} \quad -(\Sigma + \Sigma^T) = \widetilde{K}_{33} \geqslant \frac{1}{2\alpha}\widetilde{K}_{13}^T\widetilde{K}_{11}^{-1}\widetilde{K}_{13} + \frac{1}{2\beta}\widetilde{K}_{23}^T\widetilde{K}_{11}^{-1}\widetilde{K}_{23}, \tag{29}$$

because we can factorize $\widetilde{N}$ as $\widetilde{N} = \varepsilon LDL^T$ with

$$D = \begin{bmatrix} 2\alpha\widetilde{K}_{11} & \mathbf{0} & \mathbf{0} \\ \mathbf{0} & 2\beta\widetilde{K}_{11} & \mathbf{0} \\ \mathbf{0} & \mathbf{0} & D_{33} \end{bmatrix}, \quad L = \begin{bmatrix} I & \mathbf{0} & \mathbf{0} \\ \mathbf{0} & I & \mathbf{0} \\ \frac{1}{\sqrt{2}\alpha}\widetilde{K}_{13}^T\widetilde{K}_{11}^{-1} & \frac{1}{\sqrt{2}\beta}\widetilde{K}_{23}^T\widetilde{K}_{11}^{-1} & I \end{bmatrix}, \tag{30}$$

and $D_{33} = 2\widetilde{K}_{33} - \frac{1}{\alpha}\widetilde{K}_{13}^T\widetilde{K}_{11}^{-1}\widetilde{K}_{13} - \frac{1}{\beta}\widetilde{K}_{23}^T\widetilde{K}_{11}^{-1}\widetilde{K}_{23}$.

The conditions (21), (25) and (29) make the matrix $\widehat{N}$ positive semi-definite, which implies that matrix N is positive semi-definite, since for a arbitrary vector $\mathbf{y}$,

$$\mathbf{y}^T N \mathbf{y} = \mathbf{y}^T S^T \widehat{N} S \mathbf{y} = \hat{\mathbf{y}}^T \widehat{N} \hat{\mathbf{y}} \geqslant 0.$$

The matrix $\widetilde{K}_{11}^{-1}$ can be written in block matrix form as

$$\widetilde{K}_{11}^{-1} = \begin{bmatrix} \widetilde{B}_{11}^{-1} + \widetilde{B}_{11}^{-1}\widetilde{B}_{12}\widetilde{D}^{-1}\widetilde{B}_{21}\widetilde{B}_{11}^{-1} & -\widetilde{B}_{11}^{-1}\widetilde{B}_{12}\widetilde{D}^{-1} \\ -\widetilde{D}^{-1}\widetilde{B}_{21}\widetilde{B}_{11}^{-1} & \widetilde{D}^{-1} \end{bmatrix},$$

with $\widetilde{D} = \widetilde{B}_{22} - \widetilde{B}_{21}\widetilde{B}_{11}^{-1}\widetilde{B}_{12}$. The choice $\Lambda = \delta I_3$ $(\delta \in \mathscr{R})$ simplifies the algebra considerably and leads to

$$\widetilde{K}_{13}^T \widetilde{K}_{11}^{-1} \widetilde{K}_{13}^T = (1-\delta)^2 \widetilde{B}_{11}, \quad \text{and} \quad \widetilde{K}_{23}^T \widetilde{K}_{11}^{-1} \widetilde{K}_{23}^T = \delta^2 \widetilde{B}_{11}.$$

That means that the last condition in (29) together with the assumption that Σ is symmetric leads to

$$\Sigma \leqslant -\frac{[\beta(1-\delta)^2 + \alpha\delta^2]\varepsilon}{4\alpha\beta}\widetilde{B}_{11}. \tag{31}$$

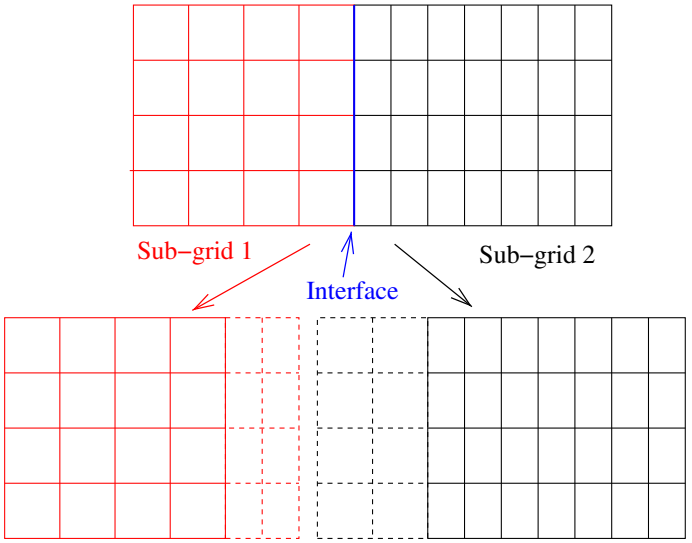

Fig. 2. Typical standard multi-block interface treatment. Layers of unknowns, here indicated by the dashed lines, are transferred between sub-grids.

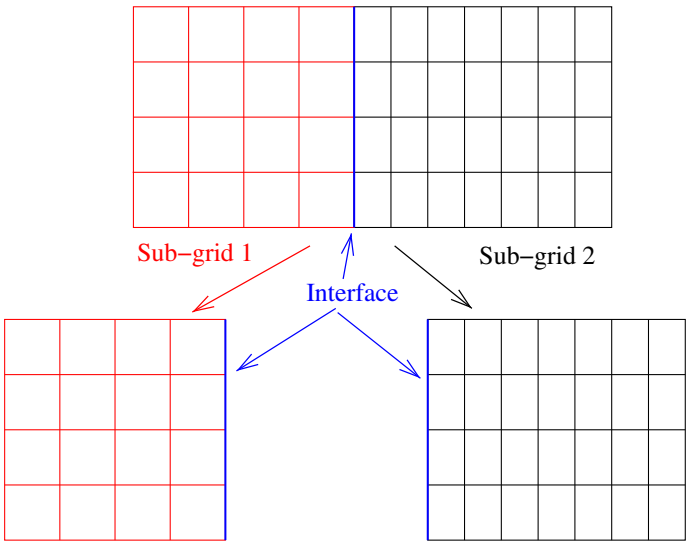

Fig. 3. Interface treatment for the current method. Only data on the interface between the two sub-grids are exchanged. Note that the nodes on the interface are duplicated. One set belongs to the left sub-grid, the other set to the right sub-grid.

Table 1
The convergence rates of density on two uniform sub-domains.

Points/block	2nd order		4th order		6th order		8th order	
	Err	q	Err	q	Err	q	Err	q
17×17	−1.29	–	−1.47	–	−1.14	–	–	–
33×33	−1.89	1.99	−2.24	2.56	−1.90	2.52	−1.89	–
65×65	−2.55	2.18	−3.14	3.00	−2.92	3.41	−3.03	3.77
129×129	−3.18	2.11	−4.12	3.24	−4.01	3.59	−4.39	4.53
257×257	−3.80	2.03	−5.06	3.15	−5.11	3.66	−5.90	5.01

Table 2
The convergence rates of density on two non-uniform sub-domains.

Points (left) + (right)	2nd order		4th order		6th order		8th order	
	Err	q	Err	q	Err	q	Err	q
$33 \times 33 + 17 \times 33$	−1.43	–	–	–	−1.30	–	−1.39	–
$65 \times 65 + 33 \times 65$	−2.02	1.94	−2.35	2.59	−2.06	2.52	−2.04	–
$129 \times 129 + 65 \times 129$	−2.65	2.09	−3.23	2.91	−3.02	3.21	−3.14	3.68
$257 \times 257 + 129 \times 257$	−3.26	2.05	−4.13	2.98	−4.09	3.53	−4.48	4.43
$513 \times 513 + 257 \times 513$	−3.88	2.05	−5.02	2.98	−5.22	3.76	−5.92	4.80

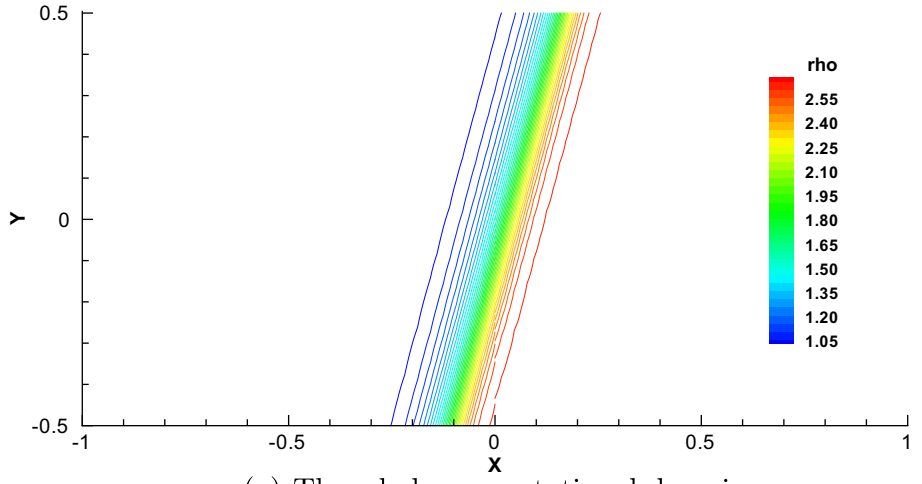

(a) The whole computational domain

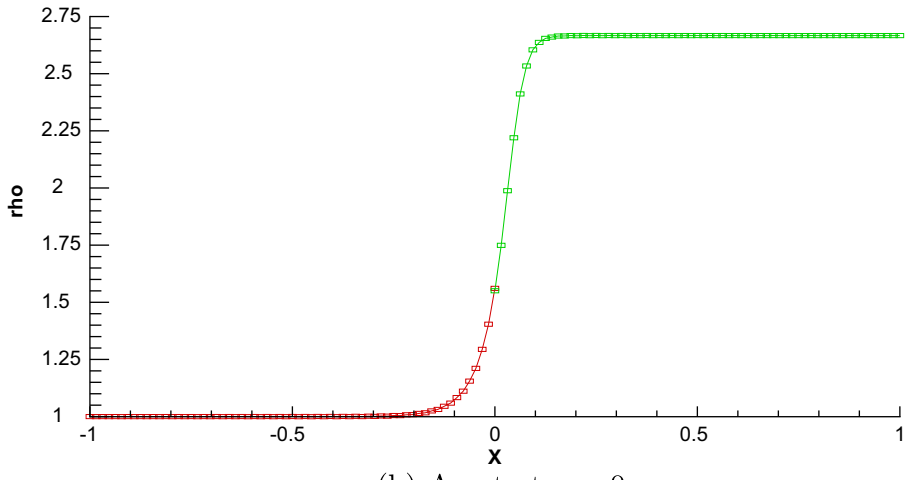

(b) A cut at $y = 0$

Fig. 4. Density isolines for a 4th order calculation. 65×65 grid points are used in both sub-domains.

It is easy to verify that the right-hand side of (31) has the least restrictive value $-\varepsilon\widetilde{B}_{11}/(4(\alpha+\beta))$ when $\delta=\beta/(\alpha+\beta)$.

Now we have done all the necessary derivations and we can summarize the result in the following proposition.

Proposition 5.1. *If the conditions*

$$\Sigma_{1I}^{L}\leqslant A_1^{-}/2 \quad (\textit{inviscid stability}), \tag{32a}$$

$$\Sigma_{1V}^{L}\leqslant -\varepsilon\widetilde{B}_{11}/4(\alpha+\beta) \quad (\textit{viscous stability}), \tag{32b}$$

$$\Sigma_{2}^{L}=-\varepsilon\beta I_4/(\alpha+\beta) \quad (\textit{viscous stability}), \tag{32c}$$

$$\Sigma_{1}^{R}=\Sigma_{1}^{L}-A_1 \quad (\textit{inviscid conservation}), \tag{32d}$$

$$\Sigma_{2}^{R}=\Sigma_{2}^{L}+\varepsilon I_4 \quad (\textit{viscous conservation}), \tag{32e}$$

are satisfied, then the scheme (15) and (16) is stable and conservative.

Remark. Recall that $\alpha=\alpha^L p^L$ and $\beta=\beta^R p^R$ $(0\leqslant\alpha^L,\beta^R\leqslant 1)$ where

$$p^L=\Delta x^L\cdot\begin{cases}\frac{1}{2} & \text{2nd order SBP},\\ \frac{17}{48} & \text{4th order SBP},\\ \frac{13{,}649}{43{,}200} & \text{6th order SBP},\end{cases}\qquad p^R=\Delta x^R\cdot\begin{cases}\frac{1}{2} & \text{2nd order SBP},\\ \frac{17}{48} & \text{4th order SBP},\\ \frac{13{,}649}{43{,}200} & \text{6th order SBP}.\end{cases}$$

In order to limit the spectral radius of the problem, the values of α^L and β^R should be chosen as large as possible, that is $\alpha^L=\beta^R=1$.

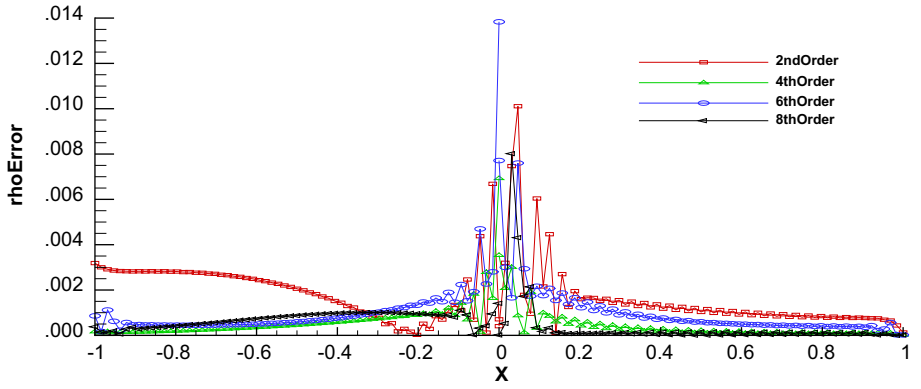

(a) 65×65 points/block

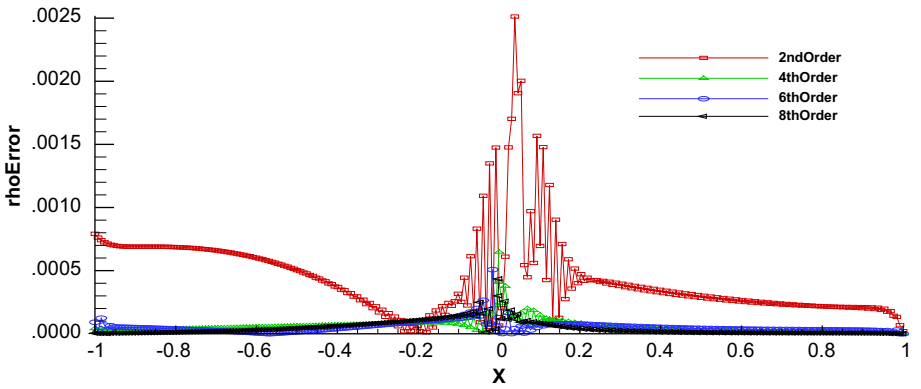

(b) 129×129 points/block

Fig. 5. The errors in density at $y=0$ with SBP operators of different orders.

Remark. Note again that the conservation conditions are a subset of the total number of stability conditions. The conditions (32e) are sufficient (but might not be necessary and unique) for a stable and conservative interface treatment.

Remark. The interface treatment do not introduce stiffness for the time integration procedure unless the penalty parameters in (32e) are increased far beyond the necessary stability limit.

5.3. Practical implementation of the interface treatment

We now illustrate how to practically implement the method. Consider the interface between two sub-grids, as shown in Fig. 1. In the more standard multi-block interface treatment typically layers of unknowns are transfered between the sub-grids, see Fig. 2, and the boundaries can be treated in the same way as internal points.

In case the grid over the interface is smooth (and the methodology is stable) this approach will give good results (even better than results obtained with the approach presented in this paper). However, in practice the grid over the interface will never be smooth (otherwise a splitting into sub-grids would not have been necessary) and will be clearly visible in the results. This is even true when a finite volume formulation is used instead of a finite difference method.

In contrast, the method presented in this work does not require the exchange of layers of unknowns; only data on the actual interface are required, see the RHS of Eqs. (15a) and (15b). Consequently, the grid over the interface does not have to be smooth in order to obtain high quality numerical solutions. The method proceeds as follows, see also Fig. 3:

1. Compute for each of the sub-grids the spatial discretization as indicated by the LHS of Eqs. (15a) and (15b). The requirements for this discretization are discussed in Section 4.
2. The solution and the viscous flux vector of the vertices located at the interface are made available to the adjacent sub-grid.
3. The RHS of Eqs. (15a) and (15b) can now be computed with the known values of the Σ's, Eq. (32e) and matrices P_x^L, P_y^L, P_x^R and P_y^R. These terms are added to the spatial residual of the boundary nodes computed in item 1.
4. The entire spatial residual is known and a time integration step can be made.

The entire procedure is repeated until the desired number of time steps is taken.

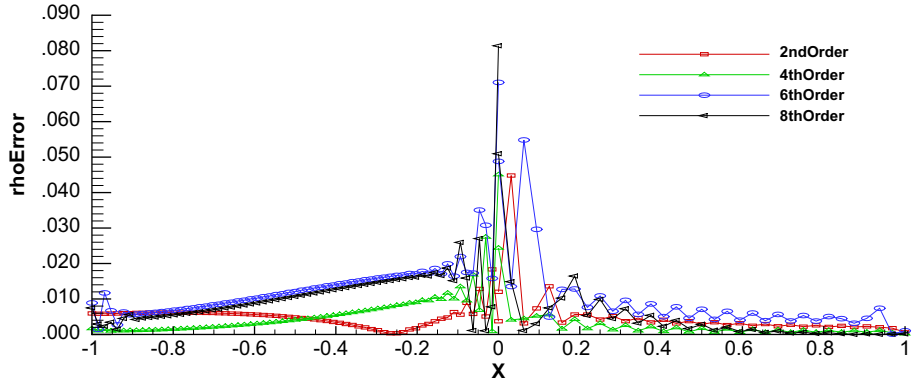

(a) $65\times65 + 33\times65$

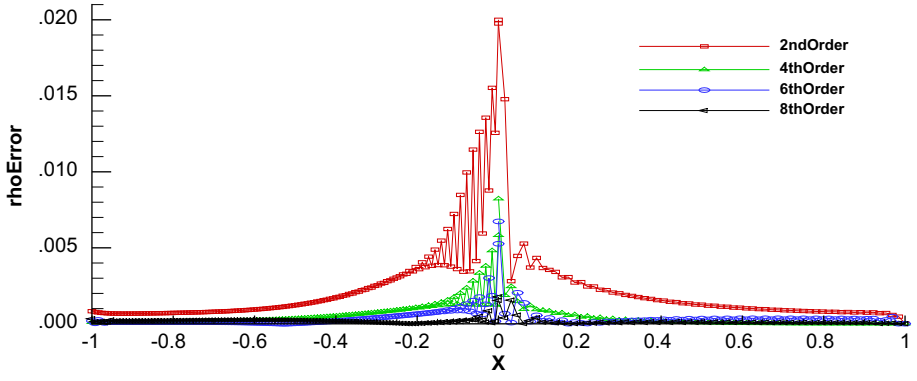

(b) $129\times129 + 65\times129$ points/block

Fig. 6. The errors in density at $y = 0$ with SBP operators of different orders.

6. Numerical experiments

The derivation of the stability and conservation properties as expressed in Proposition 5.1 was done for the constant coefficient problem. We now verify that the result of the linear analysis is valid for the full non-linear Navier–Stokes equations.

6.1. Verification of accuracy and stability of the new interface treatment

We consider a calculation on two sub-domains coupled at an interface, see Fig. 1. A stationary viscous shock problem where the middle of shock is located at the interface is calculated. This problem has an analytical solution (for Prandtl number $Pr = 3/4$) which means that we have full control of the errors. The Mach number in front of the shock in the reference frame of the shock is 2.0 and the angle of the shock relative to the Cartesian frame is 15°. The Reynolds number $Re = 50.0$ is based on the Mach number of shock. The penalty terms in (32e) are chosen by the minimum required values. We integrate the solution to steady-state using the third order low storage explicit time advancement scheme of Le and Moin [13].

In the hybrid scheme, the second derivative SBP operator is constructed with $2p$th $(p = 1, 2, \ldots)$ order accuracy internal and $(p-1)$th order at the boundary by using a diagonal norm. It was proved in [27] that if the solution is point wise bounded, the accuracy of the scheme is two orders higher than the accuracy of the second derivative approximation at the boundaries. The convergence rates for the second-, fourth-, sixth- and eighth-order schemes are thus 2, 3, 4 and 5, respectively. Since the errors for all variables (density, velocities and energy) are very similar, only the density errors are shown in our calculations. The accuracy is shown in Tables 1 and 2. The results are in agreement with the theory, see [8,9,27].

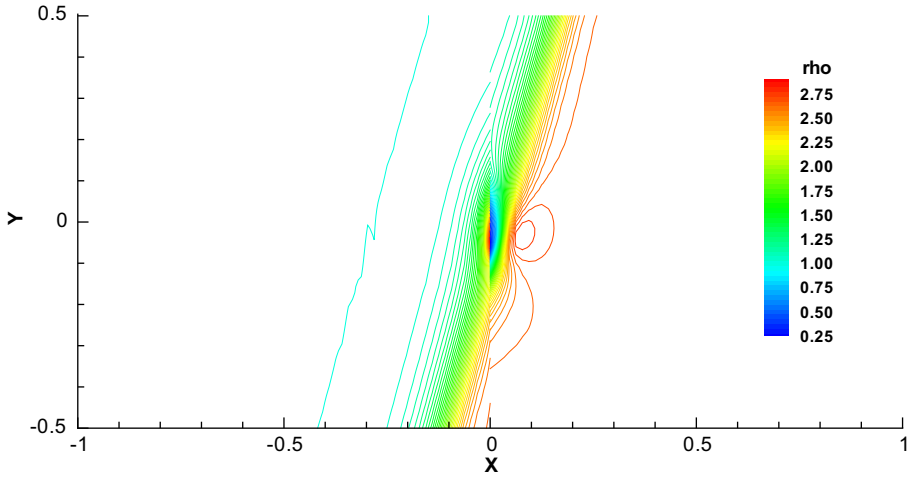

(a) The density

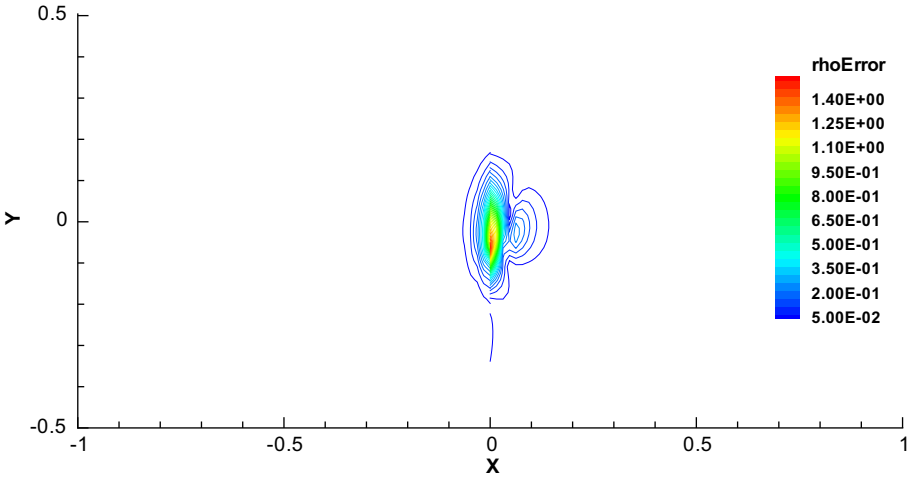

(b) The error in density

Fig. 7. A 4th order calculation without the necessary viscous penalty terms.

In the next calculation we consider the solution computed on the mesh in Fig. 1. Fig. 4(a) shows the density isolines using the 4th order discretization. The corresponding cut at $y = 0$ can be found in Fig. 4(b). The distribution of density close to the interface $x = 0$ is very smooth, which illustrates that the interface does not introduce large reflections and oscillations.

The density errors at $y = 0$ with SBP operators of different order are shown in Figs. 5 and 6. Fig. 5 shows the result for two uniform meshes, while in Fig. 6 the right block is twice as coarse in the x-direction as the left block. Figs. 5(a) and 6(a) show that the higher order schemes have rather large errors, comparable to the lower order schemes close to the interface $x = 0$ for the coarse mesh. However, when the mesh is refined, (129×129 and 65×129, respectively) the higher order schemes outperform the lower order schemes (see Figs. 5(b) and 6(b)). Tables 1 and 2 and Figs. 5 and 6 illustrate that the interface treatment is stable and accurate for all orders of accuracy.

To further illustrate the necessity of having correct penalty terms we neglect the viscous penalty term completely. This leads to a complete failure for all schemes (blow up in a couple of time steps), see Fig. 7.

6.2. Two applications using the new interface treatment

We start by demonstrating the multi-block method on a moving shock problem. The unsteady computation has been carried out on a uniform grid of 65×65 in each block in combination with the 4th order accurate SBP operator. All penalty parameters have the same values as for the previous steady case. The shock moves at Mach = 0.15 under 45°. Snapshots of the solution between $t = 0.0$ and $t = 8.0$ are shown in Fig. 8. The shape of the shock through the interface $x = 0$ remains intact, and the corresponding errors are small, see Fig. 9.

To further illustrate the performance and applicability of the new interface treatment we consider the flow around a cylinder. The Mach number is 0.1 and the Reynolds number is 100. The computational results are shown for a large time ($T = 1500$) when the initial disturbances have died out and a periodic shedding of von Karman vortices has been established,

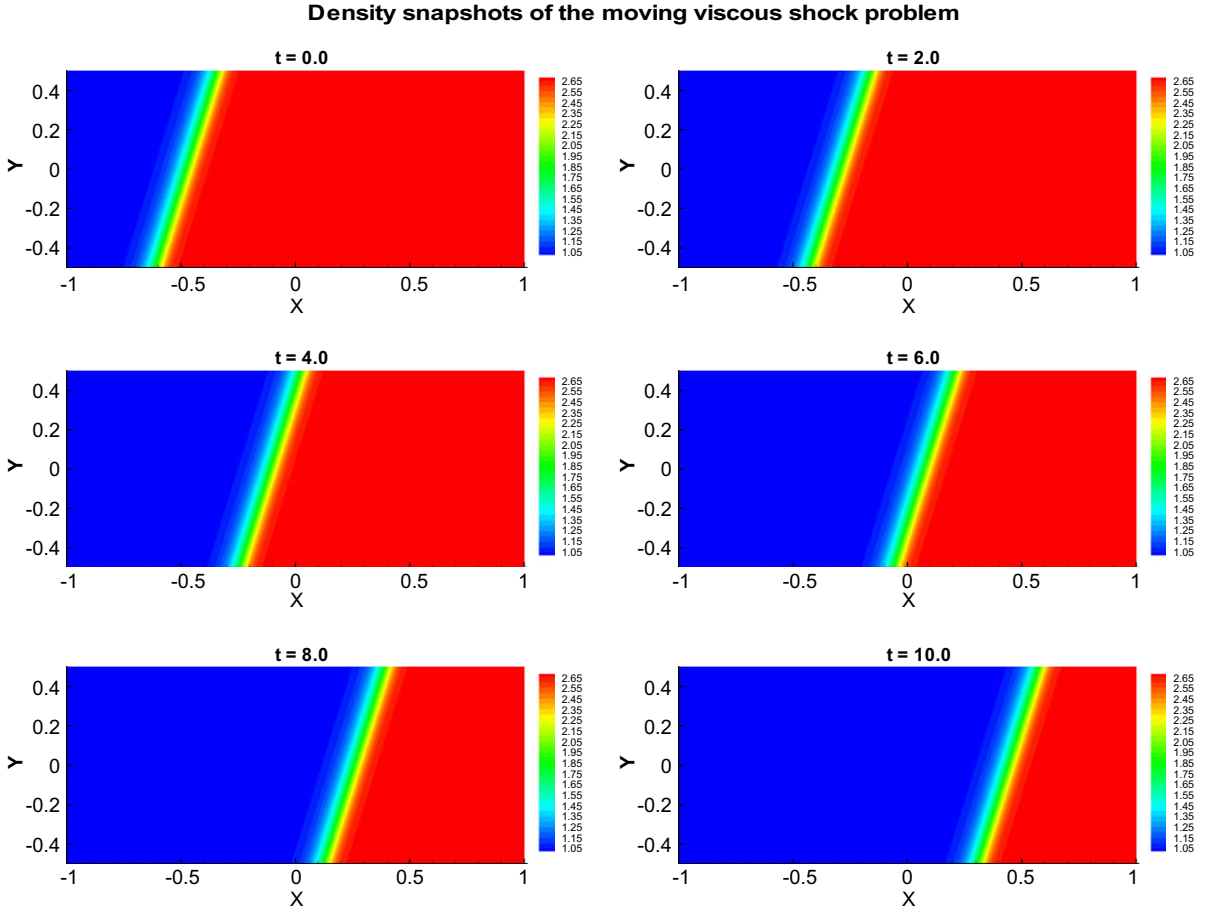

Fig. 8. Density isolines, 4th order accuracy for the unsteady shock problem.

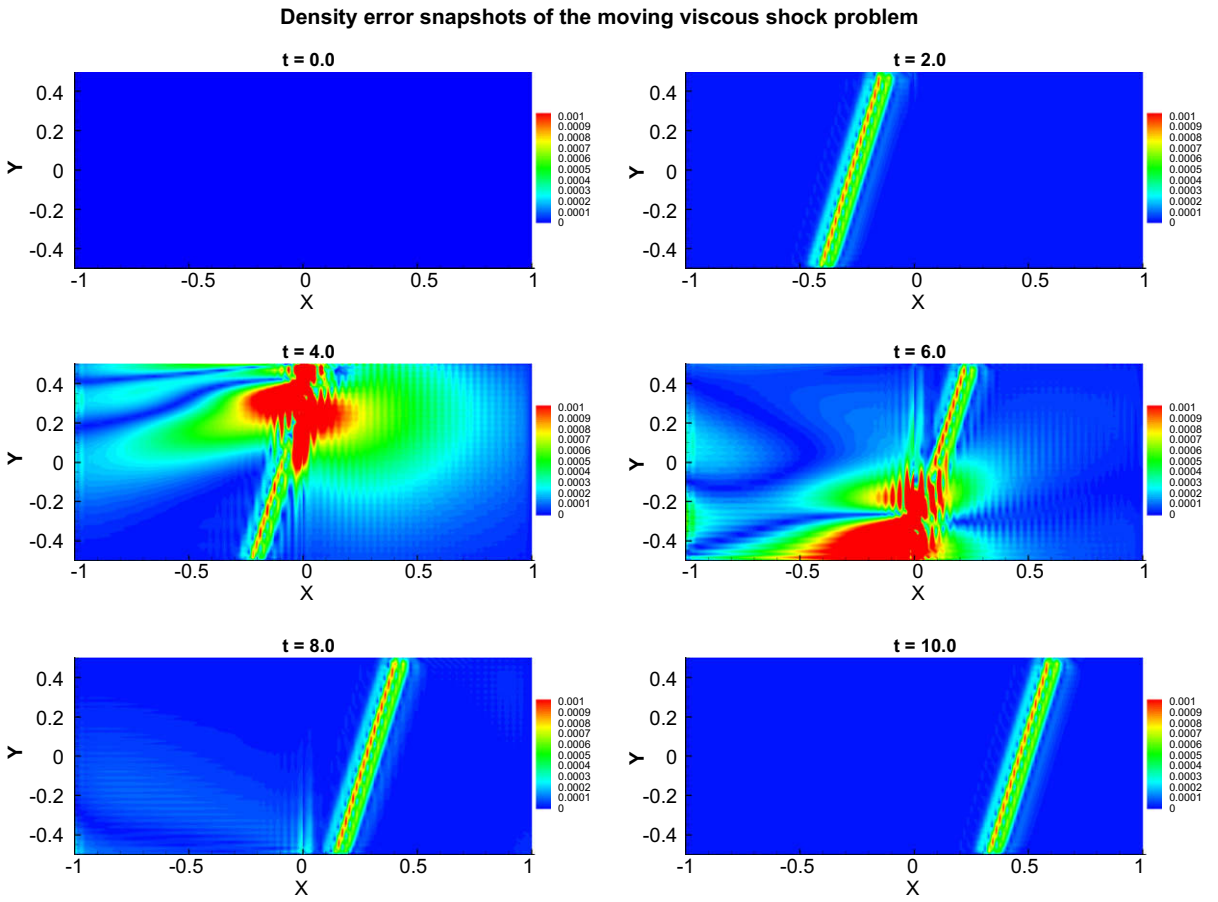

Fig. 9. The error in density, 4th order accuracy for the unsteady shock problem.

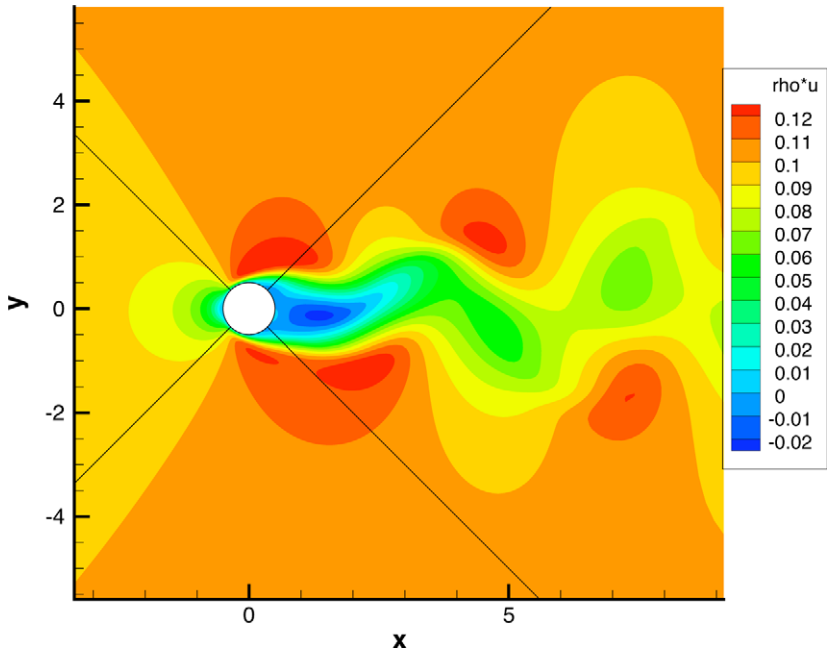

Fig. 10. A global view of 5th order accurate cylinder calculation showing the shedding of von Karman vortices. The x-momentum ρu is shown.

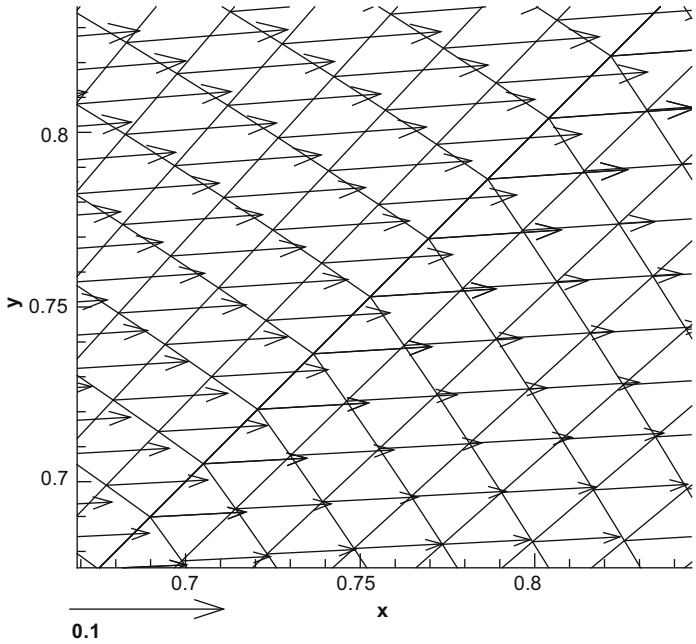

Fig. 11. A zoom in on the velocity field and the mesh close to a block interface. The velocity field is continuous over the interface, the mesh is not.

see Fig. 10. The flow field in terms of ρu is shown. The 5th order accurate method is used. We have used 5 blocks with $201 * 101$ grid points in each block (the utmost right block is not included in the figure). The global quantities such as Strouhal number, lift and drag are correctly predicted, for more details on this, see [28].

To investigate the specific topic of this paper we consider the solution close to the block interface on the upper "north east" side of the cylinder. Fig. 11 shows the velocity field and the mesh. The mesh is clearly not smooth, but the solution is.

7. Conclusions

We have proved stability and conservation of a high order accurate multi-block finite difference method applied to the Navier–Stokes equations. As theoretical tools we have used difference operators of SBP type, a penalty technique for the interface conditions and the energy method.

The stability and conservation conditions are derived without approximations. This indicates that the derived conditions are sharp. That conclusion is supported by the numerical calculations which show that instabilities occur if the conditions are violated.

Mesh refinement studies for a steady viscous shock and computations of a moving viscous shock has been performed. We also considered the flow over a cylinder. The numerical experiments support the theoretical conclusions and show that the interface coupling is stable and converge at the correct order.

References

[1] S. Abarbanel, D. Gottlieb, Optimal time splitting for two- and three-dimensional Navier–Stokes equations with mixed derivatives, Journal of Computational Physics 41 (1981) 1–43.
[2] M.J. Berger, Stability of interfaces with mesh refinement, Mathematics of Computation 45 (1985) 551–574.
[3] M.H. Carpenter, J. Nordström, D. Gottlieb, A stable and conservative interface treatment of arbitrary spatial accuracy, Journal of Computational Physics 148 (1999) 341–365.
[4] M. Darbandi, A. Naderi, Multiblock hybrid grid finite volume method to solve flow in irregular geometries, Computer Methods in Applied Mechanics and Engineering 196 (2006) 321–336.
[5] C. de Nicola, G. Pinto, R. Tognaccini, A normal mode stability analysis of multiblock algorithms for the solution of fluid-dynamics equations, Applied Numerical Mathematics 19 (1996) 419–431.
[6] L. Ferm, P. Lötstedt, Accurate and stable grid interfaces for finite volume methods, Applied Numerical Mathematics 49 (2004) 207–224.
[7] J. Gong, J. Nordström, A stable and efficient hybrid method for viscous problems in complex geometries, Journal of Computational Physics 226 (2) (2007) 1291–1309.
[8] B. Gustafsson, The convergence rate for difference approximation to mixed initial boundary value problems, Mathematics of Computation 29 (1975).
[9] B. Gustafsson, The convergence rate for difference approximation to general mixed initial boundary value problems, SIAM Journal on Numerical Analysis 18 (2) (1981) 179–190.
[10] B. Gustafsson, H.-O. Kreiss, J. Oliger, Time Dependent Problems and Difference Methods, John Wiley & Sons Inc., 1995.
[11] R.A. Horn, C.R. Johnson, Topics in Matrix Analysis, Cambridge University Press, 1991.

[12] H.-O. Kreiss, G. Scherer, Finite element and finite difference methods for hyperbolic partial differential equations, in: C. De Boor (Ed.), Mathematical Aspects of Finite Elements in Partial Differential Equation, Academic Press, New York, 1974.
[13] H. Le, P. Moin, An improvement of fractional step methods for the incompressible Navier–Stokes equations, Journal of Computational Physics 92 (1991) 369–379.
[14] A. Lerat, Z.N. Wu, Stable conservative multidomain treatments for implicit solvers, Journal of Computational Physics 123 (1995) 45–64.
[15] J. Nordström, M.H. Carpenter, Boundary and interface conditions for high order finite difference methods applied to the Euler and Navier–Stokes equations, Journal of Computational Physics 148 (1999) 621–645.
[16] J. Nordström, M.H. Carpenter, High-order finite difference methods, multidimensional linear problems and curvilinear coordinates, Journal of Computational Physics 173 (2001) 149–174.
[17] J. Nordström, J. Gong, A stable hybrid method for hyperbolic problems, Journal of Computational Physics 212 (2006) 436–453.
[18] J. Nordström, R. Gustafsson, High order finite difference approximations of electromagnetic wave propagation close to material discontinuities, Journal of Scientific Computing 18 (2) (2003) 215–234.
[19] J. Nordström, F. Ham, M. Shoeybi, E. van der Weide, M. Svärd, K. Mattsson, G. Iaccarino, J. Gong, A hybrid method for unsteady fluid flow, Computers and Fluids 38 (2009) 875–882.
[20] J. Nordström, M. Svärd, Well-posed boundary conditions for the Navier–Stokes equations, SIAM Journal on Numerical Analysis 43 (3) (2005) 1231–1255.
[21] F. Olsson, N.A. Petersson, Stability of interpolation on overlapping grids, Computers and Fluids 25 (1996) 583–605.
[22] E. Pärt-Enander, B. Sjögren, Conservative and non-conservative interpolation between overlapping grids for finite volume solutions of hyperbolic problems, Computers and Fluids 23 (1994) 551–574.
[23] A. Rizzi, P. Eliasson, I. Lindblad, C. Hirsch, C. Lacour, J. Hauser, The engineering of multiblock multi-grid software for Navier–Stokes flows on structured meshes, Computers and Fluids 22 (1993) 341–367.
[24] B. Strand, Summation by parts for finite difference approximation for d/dx, Journal of Computational Physics 110 (1) (1994) 47–67.
[25] J.C. Strickwerda, Initial boundary value problems for incompletely parabolic systems, Communications on Pure and Applied Mathematics 9 (3) (1977) 797–822.
[26] M. Svärd, M.H. Carpenter, J. Nordström, A stable high-order finite difference scheme for the compressible Navier–Stokes equations: far-field boundary conditions, Journal of Computational Physics 225 (1) (2007) 1020–1038.
[27] M. Svärd, J. Nordström, On the order of accuracy for difference approximations of initial-boundary value problems, Journal of Computational Physics 218 (1) (2006) 333–352.
[28] M. Svärd, J. Nordström, A stable high-order finite difference scheme for the compressible Navier–Stokes equations: no-slip wall boundary conditions, Journal of Computational Physics 227 (10) (2008) 4805–4824.
[29] E. van der Weide, G. Kalitzin, J. Schluter, J.J. Alonso, Unsteady turbomachinery computations using massively parallel platforms, AIAA Paper 2006-421, 2006.